

Vacuum-polarization screening corrections to the energy levels of heliumlike ions

A. N. Artemyev,^{1,2} T. Beier,³ G. Plunien,⁴ V. M. Shabaev,^{1,2} G. Soff,⁴ and V. A. Yerokhin^{1,5}

¹Max-Planck-Institut für Physik komplexer Systeme, Nöthnitzer Straße 38, D-01187 Dresden, Germany

²Department of Physics, St. Petersburg State University, Oulianovskaya 1, Petrodvorets, St. Petersburg 198904, Russia

³Fysik och Teknisk Fysik, Chalmers Tekniska Högskola och Göteborgs Universitet, SE-412 96 Göteborg, Sweden

⁴Institut für Theoretische Physik, TU Dresden, Mommsenstraße 13, D-01062 Dresden, Germany

⁵Institute for High Performance Computing and Data Bases, Fontanka 118, St. Petersburg 198005, Russia

(Received 27 October 1999; revised manuscript received 3 April 2000; published 20 July 2000)

Calculations of the vacuum-polarization screening corrections to the low-lying energy levels of He-like highly charged ions are presented. The calculations are carried out for extended nuclei in the range $Z = 20-100$.

PACS number(s): 12.20.Ds, 31.30.-i, 31.30.Jv

I. INTRODUCTION

The considerable progress in experimental investigations of multicharged ions has shown the strong necessity for accurate calculations of all the QED corrections up to second order in α (α is the fine-structure constant). In Refs. [1,2] the two-electron contribution to the ground-state energy of He-like ions was measured directly by comparing the ionization energies of heliumlike and hydrogenlike ions. In these measurements the one-electron contributions, which mainly determine the theoretical uncertainty of the energy levels, are completely eliminated. It provides good perspectives for testing the two-electron QED effects of second order in α , since at present the two-electron contribution to the ground-state energy in heliumlike ions is the only measured value which has been calculated up to second order in α . The two-electron contribution of second order in α is given by the sum of the two-photon exchange diagrams, the self-energy screening diagrams, and the vacuum polarization screening diagrams. For the ground state of heliumlike ions, a calculation of the two-photon exchange diagrams was presented in Refs. [3,4] while the self-energy screening and vacuum polarization screening diagrams were evaluated in Refs. [5-7]. Although the present experimental accuracy of the two-electron contribution [1,2] is not high enough, one can expect that it will be significantly improved in the near future. It is also expected that the corresponding experiments will be accomplished for excited states of heliumlike ions. This demonstrates that calculations of the two-electron contributions for excited states of heliumlike ions are necessary. In the present paper we start corresponding calculations by evaluating the vacuum-polarization screening corrections to the $(1s2s)_{0,1}$, $(1s2p_{1/2})_{0,1}$, and $(1s2p_{3/2})_{1,2}$ energy levels.

In the full relativistic calculations considered here the j - j coupling scheme is natural. Since the states $(1s2p_{1/2})_1$ and $(1s2p_{3/2})_1$ are strongly mixed for low and middle Z they must be treated as quasidegenerate states and, so, the off-diagonal matrix elements between these states have to be taken into account. The transition to the wave functions corresponding to the LS -coupling scheme can be performed using the equation [8]

$$\begin{pmatrix} |1s2p^3P_1\rangle \\ |1s2p^1P_1\rangle \end{pmatrix} = R \begin{pmatrix} |(1s2p_{\frac{1}{2}})_{1,1}\rangle \\ |(1s2p_{\frac{3}{2}})_{1,1}\rangle \end{pmatrix}, \quad (1)$$

where

$$R = \frac{1}{\sqrt{3}} \begin{pmatrix} \sqrt{2} & -1 \\ 1 & \sqrt{2} \end{pmatrix}. \quad (2)$$

Throughout this paper, we use relativistic units ($\hbar = c = m_e = 1$).

II. FORMULATION

Since some of the states under consideration must be treated as quasidegenerate states, we will formulate the perturbation theory for quasidegenerate levels. The case of a single level can be considered as a simple special case of this formulation. To formulate the perturbation theory for the calculation of the energy levels within QED it is convenient to use the two-time Green function (TTGF) method proposed in Ref. [9] and described in detail in Ref. [10] for a single level and in Ref. [11] for degenerate levels (in this method, the quasidegenerate levels are treated in the same way as degenerate levels). An application of the method to quasidegenerate levels was considered in Ref. [12].

Following the TTGF method to formulate the perturbation theory for the system under consideration we introduce the Fourier transform of the two-time Green function projected on the unperturbed quasidegenerate states:

$$\begin{aligned} g(E) \delta(E - E') \\ = \frac{\pi}{i} \int_{-\infty}^{\infty} dp_1^0 dp_2^0 dp_1'^0 dp_2'^0 \delta(E - p_1^0 - p_2^0) \\ \times \delta(E' - p_1'^0 - p_2'^0) P_0 G(p_1'^0, p_2'^0; p_1^0, p_2^0) \gamma_1^0 \gamma_2^0 P_0, \end{aligned} \quad (3)$$

where $P_0 = \sum_i u_i u_i^\dagger$ is the projector on the subspace of the unperturbed quasidegenerate states. The unperturbed wave functions are written as

$$u_i = \sum_{m_1 m_2} \langle j_{i_1} m_{i_1} j_{i_2} m_{i_2} | JM \rangle \frac{1}{\sqrt{2}} \sum_P (-1)^P |Pi_1 Pi_2\rangle, \quad (4)$$

where i_1 represents the $1s$ state while i_2 represents one of $2s$, $2p_{1/2}$, and $2p_{3/2}$ states; P is the permutation operator

$$\sum_P (-1)^P |Pi_1Pi_2\rangle = |i_1i_2\rangle - |i_2i_1\rangle,$$

$|i_1i_2\rangle \equiv |i_1\rangle|i_2\rangle$ is the product of the one-electron Dirac wave functions. $G(p_1^{\prime 0}, \mathbf{x}_1', p_2^{\prime 0}, \mathbf{x}_2'; p_1^0, \mathbf{x}_1, p_2^0, \mathbf{x}_2)$ is the usual “four-time” Green function in the mixed energy-coordinate representation. In the interaction representation it is given by

$$G(p_1^{\prime 0}, \mathbf{x}_1', p_2^{\prime 0}, \mathbf{x}_2'; p_1^0, \mathbf{x}_1, p_2^0, \mathbf{x}_2) = \frac{1}{(2\pi)^4} \int_{-\infty}^{\infty} dx_1^0 dx_2^0 dx_1^{\prime 0} dx_2^{\prime 0} \exp(ip_1^{\prime 0}x_1^{\prime 0} + ip_2^{\prime 0}x_2^{\prime 0} - ip_1^0x_1^0 - ip_2^0x_2^0) \times \frac{\left\langle 0 \left| T \psi_{\text{in}}(x_1') \psi_{\text{in}}(x_2') \bar{\psi}_{\text{in}}(x_2) \bar{\psi}_{\text{in}}(x_1) \exp \left\{ i \int d^4z \mathcal{L}_{\text{int}}(z) \right\} \right| 0 \right\rangle}{\left\langle 0 \left| T \exp \left\{ i \int d^4z \mathcal{L}_{\text{int}}(z) \right\} \right| 0 \right\rangle}. \quad (5)$$

Here $\psi_{\text{in}}(x)$ denotes the electron-positron field operator in the interaction representation. The Green function G is constructed by Eq. (5) according to Wick’s theorem. The Feynman rules for $G(p_1^{\prime 0}, \mathbf{x}_1', p_2^{\prime 0}, \mathbf{x}_2'; p_1^0, \mathbf{x}_1, p_2^0, \mathbf{x}_2)$ are given in Ref. [11]. It can be derived (see Ref. [11] for details) that the exact energies of the states under consideration are determined by the Schrödinger-like equation

$$H\psi_k = E_k\psi_k, \quad \psi_k^\dagger \psi_{k'} = \delta_{kk'}, \quad (6)$$

where

$$H = P^{-1/2} K P^{-1/2},$$

$$K = \frac{1}{2\pi i} \oint_{\Gamma} dE E g(E),$$

$$P = \frac{1}{2\pi i} \oint_{\Gamma} dE g(E).$$

Γ is a contour in the complex E plane which surrounds the levels under consideration and does not surround other levels, and E_k are the exact energies of the levels. It is assumed that the contour Γ is oriented anticlockwise. Substituting

$$g(E) = g^{(0)}(E) + g^{(1)}(E) + g^{(2)}(E) + \dots, \quad (7)$$

$$P = P^{(0)} + P^{(1)} + P^{(2)} + \dots, \quad (8)$$

$$K = K^{(0)} + K^{(1)} + K^{(2)} + \dots, \quad (9)$$

where the upper symbol indicates the order in α , we obtain [12]

$$H^{(0)} = K^{(0)}, \quad (10)$$

$$H^{(1)} = K^{(1)} - \frac{1}{2} P^{(1)} K^{(0)} - \frac{1}{2} K^{(0)} P^{(1)}, \quad (11)$$

$$H^{(2)} = K^{(2)} - \frac{1}{2} P^{(2)} K^{(0)} - \frac{1}{2} K^{(0)} P^{(2)} - \frac{1}{2} P^{(1)} K^{(1)} - \frac{1}{2} K^{(1)} P^{(1)} + \frac{3}{8} P^{(1)} P^{(1)} K^{(0)} + \frac{3}{8} K^{(0)} P^{(1)} P^{(1)} + \frac{1}{4} P^{(1)} K^{(0)} P^{(1)}. \quad (12)$$

The solubility of Eq. (6) yields the equation for calculation of the energy levels:

$$\det(E - H) = 0. \quad (13)$$

As was noticed in Ref. [12], due to nonzero decay rates of excited states, we should specify by H in Eqs. (6) and (13) its self-adjoint part:

$$H \equiv (1/2)(H + H^\dagger).$$

In the zeroth approximation, using the Feynman rules from Ref. [11] one easily finds

$$g^{(0)}(E) = \sum_i \frac{|u_i\rangle \langle u_i|}{E - E_i^{(0)}}, \quad (14)$$

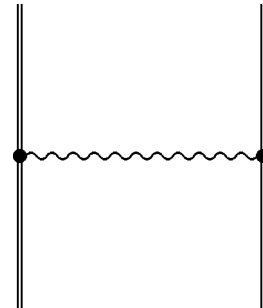


FIG. 1. One-photon exchange diagram.

where $E_i^{(0)}$ are the unperturbed energies of the states under consideration. They are equal to the sum of the one-electron Dirac-Coulomb energies:

$$E_i^{(0)} = \varepsilon_{i_1} + \varepsilon_{i_2}.$$

Substituting Eq. (14) into the definitions of K , P , and H given above, we find

$$K_{ik}^{(0)} = E_i^{(0)} \delta_{ik}, \quad (15)$$

$$P_{ik}^{(0)} = \delta_{ik}, \quad (16)$$

$$H_{ik}^{(0)} = E_i^{(0)} \delta_{ik}. \quad (17)$$

A. One-photon exchange diagram

Before deriving the contributions from the vacuum polarization screening diagrams, we consider in detail the derivation of the contribution due to the one-photon exchange diagram depicted in Fig. 1. All the derivations for higher-order contributions can be done in analogy to the derivation presented in this section. In order to compactify the formulas, we will construct the matrix elements of H between the one-determinant wave functions

$$u_i = \frac{1}{\sqrt{2}} \sum_P (-1)^P |P i_1 P i_2\rangle. \quad (18)$$

The transition to the wave functions defined by Eq. (4) can easily be accomplished in the final formulas. In what follows, we will use also the notation [10]

$$I(\omega) \equiv 4\pi\alpha\alpha_1^\mu\alpha_2^\nu D_{\mu\nu}(\omega). \quad (19)$$

Here $\alpha^\mu \equiv \gamma^0 \gamma^\mu = (1, \boldsymbol{\alpha})$, $D_{\mu\nu}$ is the photon propagator given by

$$D_{\mu\nu}(\omega, \mathbf{x} - \mathbf{y}) = g_{\mu\nu} \frac{\exp(i\sqrt{\omega^2 - \mu^2 + i0}|\mathbf{x} - \mathbf{y}|)}{4\pi|\mathbf{x} - \mathbf{y}|} \quad (20)$$

in the Feynman gauge ($\text{Im}\sqrt{\omega^2 - \mu^2 + i0} > 0$). Below we will employ the following symmetry properties of the photon propagator in Feynman gauge:

$$I(\omega) = I(-\omega),$$

$$I'(\omega) = -I'(-\omega).$$

To derive the formulas for $H_{ik}^{(1)}$ we will assume that $E_i^{(0)} \neq E_k^{(0)}$. However, all the final formulas remain to be valid also for the case $E_i^{(0)} = E_k^{(0)}$, which was considered in detail in Ref. [10]. According to the Feynman rules and the definition of $g(E)$, the contribution of the one-photon exchange diagram (Fig. 1) to $g(E)$ is

$$g_{ik}^{(1)}(E) = \left(\frac{i}{2\pi}\right)^2 \int_{-\infty}^{\infty} dp_1^0 dp_1'^0 \sum_P (-1)^P \times \frac{1}{p_1'^0 - \varepsilon_{P i_1} + i0} \frac{1}{E - p_1'^0 - \varepsilon_{P i_2} + i0} \frac{1}{p_1^0 - \varepsilon_{k_1} + i0} \frac{1}{E - p_1^0 - \varepsilon_{k_2} + i0} \langle P i_1 P i_2 | I(p_1'^0 - p_1^0) | k_1 k_2 \rangle. \quad (21)$$

Transforming

$$\frac{1}{p_1'^0 - \varepsilon_{P i_1} + i0} \frac{1}{E - p_1'^0 - \varepsilon_{P i_2} + i0} = \frac{1}{E - E_i^{(0)}} \left(\frac{1}{p_1'^0 - \varepsilon_{P i_1} + i0} + \frac{1}{E - p_1'^0 - \varepsilon_{P i_2} + i0} \right),$$

$$\frac{1}{p_1^0 - \varepsilon_{k_1} + i0} \frac{1}{E - p_1^0 - \varepsilon_{k_2} + i0} = \frac{1}{E - E_k^{(0)}} \left(\frac{1}{p_1^0 - \varepsilon_{k_1} + i0} + \frac{1}{E - p_1^0 - \varepsilon_{k_2} + i0} \right), \quad (22)$$

we obtain

$$K_{ik}^{(1)} = \frac{1}{2\pi i} \oint_{\Gamma} dE \frac{E}{(E - E_i^{(0)})(E - E_k^{(0)})} \left\{ \left(\frac{i}{2\pi}\right)^2 \times \int_{-\infty}^{\infty} dp_1^0 dp_1'^0 \sum_P (-1)^P \left(\frac{1}{p_1'^0 - \varepsilon_{P i_1} + i0} + \frac{1}{E - p_1'^0 - \varepsilon_{P i_2} + i0} \right) \times \left(\frac{1}{p_1^0 - \varepsilon_{k_1} + i0} + \frac{1}{E - p_1^0 - \varepsilon_{k_2} + i0} \right) \langle P i_1 P i_2 | I(p_1'^0 - p_1^0) | k_1 k_2 \rangle \right\}. \quad (23)$$

The expression in the curly brackets of Eq. (23) is an analytical function of E inside the contour Γ , if the photon mass μ is chosen properly (see Refs. [11,12]). This follows observing that the integrand in this expression is the sum of terms which contain singularities in p_1^0 ($p_1^{\prime 0}$) from the electron propagators only above or below the real axis. Therefore, in each term we can vary E in the complex E plane within the contour Γ keeping the same order of bypassing the singularities in the p_1^0 ($p_1^{\prime 0}$) integration by moving slightly the contour of the p_1^0 ($p_1^{\prime 0}$) integration in the com-

plex plane. The branch points of the photon propagators are moved outside the contour Γ due to the nonzero photon mass. Calculating the E residues and taking into account the identity

$$\left(\frac{i}{2\pi}\right)\left(\frac{1}{x+i0} + \frac{1}{-x+i0}\right) = \delta(x) \quad (24)$$

we obtain

$$K_{ik}^{(1)} = \frac{i}{2\pi} \int_{-\infty}^{\infty} dp_1^0 \sum_P (-1)^P \frac{E_i^{(0)} \langle Pi_1 Pi_2 | I(\varepsilon_{p_{i_1} - p_1^0}) | k_1 k_2 \rangle}{E_i^{(0)} - E_k^{(0)}} \left(\frac{1}{p_1^0 - \varepsilon_{k_1} + i0} + \frac{1}{E_i^{(0)} - p_1^0 - \varepsilon_{k_2} + i0} \right) + \frac{i}{2\pi} \int_{-\infty}^{\infty} dp_1^{\prime 0} \sum_P (-1)^P \frac{E_k^{(0)} \langle Pi_1 Pi_2 | I(p_1^{\prime 0} - \varepsilon_{k_1}) | k_1 k_2 \rangle}{E_k^{(0)} - E_i^{(0)}} \left(\frac{1}{p_1^{\prime 0} - \varepsilon_{p_{i_1}} + i0} + \frac{1}{E_k^{(0)} - p_1^{\prime 0} - \varepsilon_{p_{i_2}} + i0} \right). \quad (25)$$

In the same way we find

$$P_{ik}^{(1)} = \frac{i}{2\pi} \int_{-\infty}^{\infty} dp_1^0 \sum_P (-1)^P \frac{\langle Pi_1 Pi_2 | I(\varepsilon_{p_{i_1} - p_1^0}) | k_1 k_2 \rangle}{E_i^{(0)} - E_k^{(0)}} \left(\frac{1}{p_1^0 - \varepsilon_{k_1} + i0} + \frac{1}{E_i^{(0)} - p_1^0 - \varepsilon_{k_2} + i0} \right) + \frac{i}{2\pi} \int_{-\infty}^{\infty} dp_1^{\prime 0} \sum_P (-1)^P \frac{\langle Pi_1 Pi_2 | I(p_1^{\prime 0} - \varepsilon_{k_1}) | k_1 k_2 \rangle}{E_k^{(0)} - E_i^{(0)}} \left(\frac{1}{p_1^{\prime 0} - \varepsilon_{p_{i_1}} + i0} + \frac{1}{E_k^{(0)} - p_1^{\prime 0} - \varepsilon_{p_{i_2}} + i0} \right). \quad (26)$$

Equations (25), (26) can easily be transformed to yield

$$K_{ik}^{(1)} = \sum_P (-1)^P \left\{ \frac{1}{2} [\langle Pi_1 Pi_2 | I(\Delta_1) | k_1 k_2 \rangle + \langle Pi_1 Pi_2 | I(\Delta_2) | k_1 k_2 \rangle] - \frac{(E_i^{(0)} + E_k^{(0)})}{2} \frac{i}{2\pi} \int_{-\infty}^{\infty} d\omega \langle Pi_1 Pi_2 | I(\omega) | k_1 k_2 \rangle \times \left[\frac{1}{(\omega + \Delta_1 - i0)(\omega - \Delta_2 - i0)} + \frac{1}{(\omega + \Delta_2 - i0)(\omega - \Delta_1 - i0)} \right] \right\}, \quad (27)$$

$$P_{ik}^{(1)} = - \sum_P (-1)^P \frac{i}{2\pi} \int_{-\infty}^{\infty} d\omega \langle Pi_1 Pi_2 | I(\omega) | k_1 k_2 \rangle \times \left[\frac{1}{(\omega + \Delta_1 - i0)(\omega - \Delta_2 - i0)} + \frac{1}{(\omega + \Delta_2 - i0)(\omega - \Delta_1 - i0)} \right], \quad (28)$$

where $\Delta_1 = \varepsilon_{p_{i_1}} - \varepsilon_{k_1}$ and $\Delta_2 = \varepsilon_{p_{i_2}} - \varepsilon_{k_2}$. Substituting Eqs. (27), (28) into (11), we get [12,13]

$$H_{ik}^{(1)} = \frac{1}{2} \sum_P (-1)^P [\langle Pi_1 Pi_2 | I(\Delta_1) | k_1 k_2 \rangle + \langle Pi_1 Pi_2 | I(\Delta_2) | k_1 k_2 \rangle]. \quad (29)$$

The numerical results for the one-photon exchange corrections are given in Tables I and II. The calculations are performed in the Feynman gauge for the Fermi distribution of the nuclear charge density,

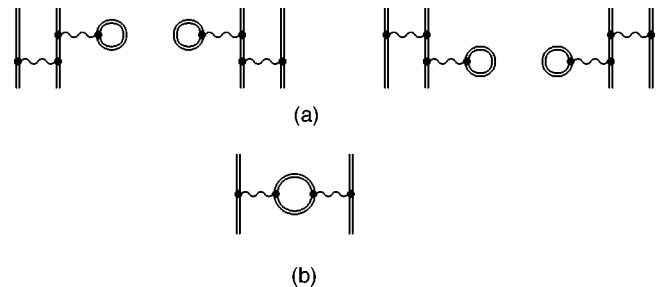


FIG. 2. Vacuum-polarization screening diagrams.

TABLE I. One-photon exchange corrections for the $(1s)^2$ and $(1s2s)_{0,1}$ states of heliumlike ions. Energies are given in eV.

Z	$\langle r^2 \rangle^{1/2}$ [fm]	$\Delta E_{(1s)^2}$	$\Delta E_{(1s2s)_0}$	$\Delta E_{(1s2s)_1}$
20	3.478	345.7624(1)	128.1561	103.1786
28	3.769	491.7688(2)	182.1657(1)	145.6921(1)
30	3.928	529.4192(2)	196.0818(1)	156.5069(1)
32	4.072	567.6094(2)	210.1937(1)	167.4096(1)
40	4.270	726.6361(5)	268.9289(1)	212.0456(1)
47	4.542	875.7531(1)	324.0087(2)	252.7450(2)
50	4.655	943.092(1)	348.9013(3)	270.7578(2)
54	4.787	1036.558(2)	383.4892(5)	295.3904(3)
60	4.914	1185.725(4)	438.8212(9)	333.8499(5)
66	5.224	1347.448(7)	499.072(2)	374.443(1)
70	5.317	1463.43(1)	542.497(3)	402.905(1)
74	5.373	1586.93(2)	588.968(4)	432.664(2)
79	5.437	1753.36(2)	652.038(7)	471.960(3)
80	5.467	1788.43(3)	665.398(8)	480.130(4)
82	5.505	1860.51(3)	692.942(9)	496.812(4)
83	5.533	1897.558(4)	707.146(1)	505.3314(6)
90	5.802	2178.06(7)	815.73(2)	568.70(1)
92	5.860	2265.88(1)	850.135(4)	588.170(2)
100	5.886	2659.8(2)	1006.98(6)	673.62(3)

$$\rho(r) = \frac{N}{1 + \exp[(r-c)/a]} \quad (30)$$

The parameter a is chosen to be $a = 2.30/(4 \ln 3)$ fm [14]. The parameter c , to a very high accuracy, is calculated by the formula (see, e.g., Ref. [15])

$$c = \sqrt{(5/3)\langle r^2 \rangle - (7/3)a^2 \pi^2}. \quad (31)$$

The values of the root-mean-square (rms) charge radii are taken from [14,16–18]. Except for $Z = 83, 92$, the uncertainties indicated in the tables are obtained by a 1% variation of the root-mean-square charge radii. In the case of $Z = 92$ ($\langle r^2 \rangle^{1/2} = 5.860(2)$ fm [18]), the uncertainty is estimated by taking the difference between the corrections obtained with the Fermi model and the homogeneously charged sphere model of the same rms radius [19]. For $Z = 83$, the uncertainty results from both a variation of the rms radius by 0.020 fm (it corresponds to a discrepancy between the measured rms values [14]) and the difference between the Fermi model and the homogeneously charged sphere model. If no error margin is specified, it is smaller than the last digit given. The fundamental constants used in the calculation are $hcR_\infty = 13.6056981(40)$ eV and $\alpha = 1/137.0359895(61)$.

In the calculation of the off-diagonal matrix elements, the one-electron wave functions of the $2p_{1/2}$ and $2p_{3/2}$ states are chosen to have the same overall sign in the nonrelativistic limit since only these functions must be used in the transition to the LS coupling according to Eq. (1). It should also be noted, that the off-diagonal matrix elements are gauge dependent. However, the relative value of the difference between the off-diagonal elements calculated in the Feynman and the Coulomb gauges amounts to 2×10^{-5} for $Z = 100$ and decreases with decreasing Z . Since our calculations are performed in the Feynman gauge, strictly speaking, all the other contributions to H must be taken in the Feynman gauge as well.

TABLE II. One-photon exchange corrections for the $(1s2p_{1/2})_{0,1}$, $(1s2p_{3/2})_{1,2}$ states of heliumlike ions. For the $(1s2p_{1/2})_1$ and $(1s2p_{3/2})_1$ states, the values $\Delta E_{(1s2p_{1/2})_1}$ and $\Delta E_{(1s2p_{3/2})_1}$ denote the matrix elements of H [see Eq. (6)] while $\Delta E_{\text{off-diag}}$ is the off-diagonal one. Energies are given in eV.

Z	$\Delta E_{(1s2p_{1/2})_0}$	$\Delta E_{(1s2p_{3/2})_2}$	$\Delta E_{(1s2p_{1/2})_1}$	$\Delta E_{(1s2p_{3/2})_1}$	$\Delta E_{\text{off-diag}}$
20	125.4308	123.3179	130.5997	135.8537	8.4614
28	179.1726(1)	173.2765(1)	184.9931(1)	191.0340(1)	11.4485
30	193.1468(1)	185.8575(1)	198.9164(1)	204.9521(1)	12.1381
32	207.3761(1)	198.4806(1)	212.9935(1)	218.9274(1)	12.8014
40	267.2805(1)	249.4501(1)	271.1035(1)	275.4821(1)	15.1592
47	324.5246(1)	294.7776(1)	324.8604(1)	325.9821(1)	16.7746
50	350.7490(1)	314.4434(1)	348.9185(1)	347.9638(1)	17.3214
54	387.5573(2)	340.9109(1)	382.1069(2)	377.6260(1)	17.9023(1)
60	447.3335(3)	381.1872(2)	434.6406(2)	422.9528(1)	18.4325(1)
66	513.6557(6)	422.2220(3)	491.1218(4)	469.3965(2)	18.5200(2)
70	562.2258(9)	450.0408(4)	531.4035(5)	501.0470(2)	18.3139(3)
74	614.893(1)	478.2588(6)	574.1586(8)	533.2967(2)	17.8842(4)
79	687.473(2)	514.1333(8)	631.678(1)	574.5172(2)	17.0176(5)
80	703.006(3)	521.3926(9)	643.797(2)	582.8892(2)	16.7990(6)
82	735.200(3)	536.000(1)	668.717(2)	599.7667(2)	16.3150(7)
83	751.8900(5)	543.3484(2)	681.5365(4)	608.2736(2)	16.0496(1)
90	881.455(8)	595.675(2)	778.992(5)	669.1577(3)	13.742(1)
92	923.198(1)	610.9271(4)	809.7047(9)	687.0034(2)	12.9340(2)
100	1117.49(3)	673.433(4)	949.20(2)	760.5393(4)	9.008(3)

B. Vacuum-polarization screening diagrams

Let us now consider the vacuum-polarization screening diagrams in Fig. 2. The contributions of these diagrams to $H_{ik}^{(2)}$ can be derived in the same way as for the one-photon exchange diagram. However, the simplest way to derive the formulas consists in using the fact that the diagrams shown in Fig. 2(a) can be obtained as the first-order correction in the vacuum polarization potential to the one-photon exchange contribution derived above while the diagram shown in Fig. 2(b) is obtained from the one-photon exchange diagram by modifying the photon propagator. So, to find the contribution from the diagrams shown in Fig. 2(a) we make the following replacements in Eq. (29):

$$|k_1\rangle \rightarrow |k_1\rangle + \delta|k_1\rangle, \quad (32)$$

$$|k_2\rangle \rightarrow |k_2\rangle + \delta|k_2\rangle, \quad (33)$$

$$|Pi_1\rangle \rightarrow |Pi_1\rangle + \delta|Pi_1\rangle, \quad (34)$$

$$|Pi_2\rangle \rightarrow |Pi_2\rangle + \delta|Pi_2\rangle, \quad (35)$$

$$I(\varepsilon_a - \varepsilon_b) \rightarrow I(\varepsilon_a + \delta\varepsilon_a - \varepsilon_b - \delta\varepsilon_b), \quad (36)$$

where to first order in the vacuum polarization potential

$$\delta|a\rangle = \sum_n^{\varepsilon_n \neq \varepsilon_a} \frac{|n\rangle \langle n| U_{VP}^a |a\rangle}{\varepsilon_a - \varepsilon_n}, \quad (37)$$

$$\delta\varepsilon_a = \langle a| U_{VP}^a |a\rangle, \quad (38)$$

The vacuum-polarization potential is given by

$$U_{VP}^a(\mathbf{x}) = \frac{\alpha}{2\pi i} \int d\mathbf{y} \frac{1}{|\mathbf{x}-\mathbf{y}|} \int_{-\infty}^{\infty} d\omega \text{Tr}[G(\omega, \mathbf{y}, \mathbf{y})], \quad (39)$$

where $G(\omega, \mathbf{x}, \mathbf{y}) = \sum_n \psi(\mathbf{x}) \psi^\dagger(\mathbf{y}) / [\omega - \varepsilon_n(1 - i0)]$ is the Coulomb Green function. Decomposing the modified expression for the one-photon exchange diagram to the first order in the vacuum polarization potential we find that the contribution from the diagrams shown in Fig. 2(a) is the sum of the irreducible and reducible parts

$$H_{ik} = H_{ik}^{(2a, \text{irred})} + H_{ik}^{(2a, \text{red})}, \quad (40)$$

where

$$\begin{aligned} H_{ik}^{(2a, \text{irred})} = & \frac{1}{2} \sum_P (-1)^P [\langle \delta Pi_1 Pi_2 | I(\Delta_1) + I(\Delta_2) | k_1 k_2 \rangle \\ & + \langle Pi_1 \delta Pi_2 | I(\Delta_1) + I(\Delta_2) | k_1 k_2 \rangle \\ & + \langle Pi_1 Pi_2 | I(\Delta_1) + I(\Delta_2) | \delta k_1 k_2 \rangle \\ & + \langle Pi_1 Pi_2 | I(\Delta_1) + I(\Delta_2) | k_1 \delta k_2 \rangle], \end{aligned} \quad (41)$$

and

$$\begin{aligned} H_{ik}^{(2a, \text{red})} = & \frac{1}{2} \sum_P (-1)^P \{ [\langle Pi_1 | U_{VP}^a | Pi_1 \rangle - \langle k_1 | U_{VP}^a | k_1 \rangle] \\ & \times \langle Pi_1 Pi_2 | I'(\Delta_1) | k_1 k_2 \rangle + [\langle Pi_2 | U_{VP}^a | Pi_2 \rangle \\ & - \langle k_2 | U_{VP}^a | k_2 \rangle] \langle Pi_1 Pi_2 | I'(\Delta_2) | k_1 k_2 \rangle \}. \end{aligned} \quad (42)$$

The contribution of the diagram shown in Fig. 2(b) is obtained from the expression (29) by the replacement of $I(\varepsilon)$ with

$$\begin{aligned} U_{VP}^b(\varepsilon, \mathbf{x}, \mathbf{y}) = & \frac{\alpha^2}{2\pi i} \int_{-\infty}^{\infty} d\omega \int d\mathbf{z}_1 \int d\mathbf{z}_2 \\ & \times \frac{\alpha_{1\mu} \exp(i|\varepsilon||\mathbf{x}-\mathbf{z}_1|)}{|\mathbf{x}-\mathbf{z}_1|} \frac{\alpha_{2\nu} \exp(i|\varepsilon||\mathbf{y}-\mathbf{z}_2|)}{|\mathbf{y}-\mathbf{z}_2|} \\ & \times \text{Tr} \left[\alpha^\mu G \left(\omega - \frac{\varepsilon}{2}, \mathbf{z}_1, \mathbf{z}_2 \right) \alpha^\nu \right. \\ & \left. \times G \left(\omega + \frac{\varepsilon}{2}, \mathbf{z}_2, \mathbf{z}_1 \right) \right]. \end{aligned} \quad (43)$$

Thus, we have

$$\begin{aligned} H_{ik}^{(2b)} = & \frac{1}{2} \sum_P (-1)^P [\langle Pi_1 Pi_2 | U_{VP}^b(\Delta_1) | k_1 k_2 \rangle \\ & + \langle Pi_1 Pi_2 | U_{VP}^b(\Delta_2) | k_1 k_2 \rangle]. \end{aligned} \quad (44)$$

Equations (41), (42), and (44) provide the matrix elements between the one-determinant wave functions defined by Eq. (18). To get the matrix elements between the wave functions defined by Eq. (4), we have to multiply these equations with the Clebsch-Gordan coefficients and sum over projections of the one-electron angular momenta.

Contributions (41), (42), and (44) are ultraviolet divergent. The renormalization of these contributions is performed in the same way as in Refs. [6,20].

III. CALCULATION

The calculation of contributions (41), (42), and (44) is performed in the same way as in our previous papers [6,20]. The formulas for the Uehling and the Wichmann-Kroll potentials in the case of the diagrams shown in Fig. 2(a) are well known:

$$\begin{aligned} U_{\text{Ueh}}^a(r) = & -\alpha Z \frac{2\alpha}{3\pi} \int_0^\infty dr' 4\pi r' \rho(r') \int_1^\infty dt \left(1 + \frac{1}{t^2} \right) \\ & \times \frac{\sqrt{t^2-1} \{ \exp(-2m|r-r'|t) - \exp[-2m(r+r')t] \}}{t^2 4mrt}, \end{aligned} \quad (45)$$

TABLE III. Vacuum-polarization screening corrections for the $(1s)^2$ and $(1s2s)_{0,1}$ states of heliumlike ions. Energies are given in eV.

Z	$\Delta E_{(1s)^2}$	$\Delta E_{(1s2s)_0}$	$\Delta E_{(1s2s)_1}$
20	0.0100	0.0021	0.0014
28	0.0298	0.0061	0.0039
30	0.0348	0.0076	0.0048
32	0.0427	0.0093	0.0058
40	0.0887	0.0199	0.0118
47	0.1610	0.0354	0.0202
50	0.1920	0.0447	0.0250
54	0.2550	0.0602	0.0328
60	0.3800(1)	0.0923	0.0484
66	0.5570(1)	0.1393	0.0702
70	0.7130(2)	0.1819	0.0893
74	0.9080(2)	0.2372	0.1133
79	1.2330(3)	0.3296(1)	0.1523
80	1.2980(3)	0.3520(1)	0.1615(1)
82	1.4660(4)	0.4014(2)	0.1817(1)
83	1.5500(7)	0.4286(2)	0.1927(2)
90	2.338(1)	0.6810(3)	0.2921(2)
92	2.630(2)	0.7770(4)	0.3287(3)
100	4.248(4)	1.3404(8)	0.5366(5)

$$\begin{aligned}
U_{\text{WK}}^a(x) = & \frac{2\alpha}{\pi} \sum_{\kappa=\pm 1}^{\pm\infty} |\kappa| \int_0^\infty d\omega \int_0^\infty dy y^2 \int_0^\infty dz z^2 \\
& \times \frac{1}{\max(x,y)} V(z) \sum_{i,k=1}^2 \text{Re}\{F_\kappa^{ik}(i\omega, y, z) \\
& \times [G_\kappa^{ik}(i\omega, y, z) - F_\kappa^{ik}(i\omega, y, z)]\}, \quad (46)
\end{aligned}$$

where V is the nuclear potential, ρ is nuclear charge density, and G_κ^{ik} and F_κ^{ik} are the radial components of the partial-wave contributions to the bound and free electron Green functions, respectively.

For the Uehling contribution, a Fermi-like nuclear charge distribution is assumed. The wave function and the reduced Green function for this charge distribution are obtained using the B -spline method for solving the Dirac equation [21]. The remaining Wichmann-Kroll potential charge density is calculated for a spherical shell model of the nuclear charge distribution. For this model, the exact solutions for the radial components of the Green function can be employed [22].

TABLE IV. Vacuum-polarization screening corrections for the $(1s2p_{1/2})_{0,1}$, $(1s2p_{3/2})_{1,2}$ states of heliumlike ions. For the $(1s2p_{1/2})_1$ and $(1s2p_{3/2})_1$ states, the values $\Delta E_{(1s2p_{1/2})_1}$ and $\Delta E_{(1s2p_{3/2})_1}$ denote the diagonal matrix elements of H [see Eq. (6)] while $\Delta E_{\text{off-diag}}$ is the off-diagonal one. Energies are given in eV.

Z	$\Delta E_{(1s2p_{1/2})_0}$	$\Delta E_{(1s2p_{3/2})_2}$	$\Delta E_{(1s2p_{1/2})_1}$	$\Delta E_{(1s2p_{3/2})_1}$	$\Delta E_{\text{off-diag}}$
20	0.0006	0.0006	0.0004	0.0001	0.0004
28	0.0017	0.0015	0.0011	0.0004	0.0010
30	0.0022	0.0019	0.0013	0.0005	0.0012
32	0.0027	0.0023	0.0017	0.0006	0.0015
40	0.0060	0.0044	0.0036	0.0012	0.0029
47	0.0110	0.0073	0.0067	0.0019	0.0048
50	0.0141	0.0089	0.0086	0.0024	0.0058
54	0.0195	0.0113	0.0119	0.0031	0.0074
60	0.0312	0.0159	0.0190	0.0044	0.0105
66	0.0494	0.0219	0.0302	0.0062	0.0144
70	0.0669	0.0267	0.0410	0.0075	0.0176
74	0.0906	0.0324	0.0556	0.0092	0.0213
79	0.1324	0.0409	0.0814	0.0115	0.0269
80	0.1429	0.0428	0.0879	0.0120	0.0281
82	0.1666(1)	0.0468	0.1026	0.0130	0.0308
83	0.1799(1)	0.0489	0.1109(1)	0.0136	0.0321
90	0.3112(2)	0.0663	0.1929(1)	0.0176	0.0433
92	0.3647(3)	0.0721	0.2262(2)	0.0188	0.0471
100	0.7067(6)	0.1009(1)	0.4408(5)	0.0234	0.0649

The contribution of the diagram shown in Fig. 2(b) is also divided into two parts: the leading (Uehling) contribution and the remaining (Wichmann-Kroll) term. The expression for the Uehling operator reads

$$\begin{aligned}
U_{\text{Uehl}}^b(\varepsilon, \mathbf{x}, \mathbf{y}) = & \alpha \frac{\alpha_{1\mu} \alpha_2^\mu}{|\mathbf{x}-\mathbf{y}|} \frac{2\alpha}{3\pi} \int_1^\infty dt \left(1 + \frac{1}{2t^2}\right) \frac{\sqrt{t^2-1}}{t^2} \\
& \times \exp(-\sqrt{(2mt)^2 - \varepsilon^2} |\mathbf{x}-\mathbf{y}|), \quad (47)
\end{aligned}$$

where ε is the energy of the transmitted photon. This contribution is also calculated using the Fermi-like nuclear charge distribution.

The Wichmann-Kroll contribution to the diagram in Fig. 2(b) is calculated utilizing the partial differences between expression (43) and the corresponding equation with the bound-electron Green functions replaced by those of free electrons. In this calculation some large terms appear which almost cancel each other. To avoid a loss of precision caused by this cancellation we employ the same procedure as in Refs. [6,20]. We divide the product of two relativistic Coulomb Green functions contained in the vacuum polarization loop into two parts, each containing only even or only odd

powers of the nuclear charge Z .¹ According to the Furry theorem, only the part containing even powers of Z is used in the calculation. This contribution is calculated for the point-nucleus case. The finite-size effects on this contribution can be neglected due to its smallness compared to the other contributions.

The numerical results of our calculation of the vacuum-polarization screening diagrams are presented in Tables III and IV. In the second column of Table III we also list the results from Ref. [6] for the ground state.² The values of the root-mean-square charge radii used in the calculation are the same as those in Table I.

¹In Ref. [6] this procedure was applied for the zero energy of the transmitted photon, and in Ref. [20] it was extended to the case of arbitrary photon energy.

²For $Z=90$ we recalculated δE_{1s}^1 with $\langle r^2 \rangle^{1/2}=5.802$ fm [18] (in Ref. [6] $\langle r^2 \rangle^{1/2}=5.645$ fm was used).

IV. CONCLUSION

In this paper we derived calculation formulas for the one-photon exchange and vacuum polarization screening diagrams in the case of quasidegenerate states of He-like ions. The calculations of corrections to the energy levels of He-like ions due to these diagrams were performed for the Fermi-like nuclear charge distribution. Calculations of the self-energy screening and two-photon exchange diagrams remain to be accomplished to obtain the total two-electron contribution up to second order in α for excited states of He-like ions.

ACKNOWLEDGMENTS

The work of A.N.A., V.M.S., and V.A.Y. was supported by the Russian Foundation for Basic Research (Grant No. 98-02-18350) and by the program Russian Universities Basic Research (Project No. 3930). T.B., G.P., V.M.S., and G.S. acknowledge support by BMBF, by GSI, and by DFG. T.B. is grateful to the EU-TMR program (Contract No. ERB FMRX CT 97-0144).

-
- [1] R. E. Marrs, S. R. Elliott, and Th. Stöhlker, *Phys. Rev. A* **52**, 3577 (1995).
- [2] Th. Stöhlker, S. R. Elliott, and R. E. Marrs, *Hyperfine Interact.* **99**, 217 (1996).
- [3] S. Blundell, P. Mohr, W. Johnson, and J. Sapirstein, *Phys. Rev. A* **48**, 2615 (1993).
- [4] I. Lindgren, H. Persson, S. Salomonson, and L. Labzowsky, *Phys. Rev. A* **51**, 1167 (1995).
- [5] V. A. Yerokhin, A. N. Artemyev, and V. M. Shabaev, *Phys. Lett. A* **234**, 361 (1997).
- [6] A. N. Artemyev, V. M. Shabaev, and V. A. Yerokhin, *Phys. Rev. A* **56**, 3529 (1997).
- [7] H. Persson, S. Salomonson, P. Sunnergren, and I. Lindgren, *Phys. Rev. Lett.* **76**, 204 (1996); H. Persson, S. Salomonson, P. Sunnergren, I. Lindgren, and M. G. H. Gustavsson, *Hyperfine Interact.* **108**, 3 (1997); P. Sunnergren, Doctoral thesis, Göteborg University and Chalmers University of Technology, Göteborg, 1998.
- [8] G. W. Drake, *Can. J. Phys.* **66**, 586 (1988).
- [9] V. M. Shabaev, in *Many-Particle Effects in Atoms*, edited by U. I. Safronova (AN SSSR, Nauchnyi Sovet po Spektroskopii, Moscow, 1988), p. 15; *Sov. Phys. J.* **33**, 660 (1990).
- [10] V. M. Shabaev and I. G. Fokeeva, *Phys. Rev. A* **49**, 4489 (1994).
- [11] V. M. Shabaev, *Phys. Rev. A* **50**, 4521 (1994).
- [12] V. M. Shabaev, *J. Phys. B* **26**, 4703 (1993).
- [13] M. H. Mittleman, *Phys. Rev. A* **5**, 2395 (1972).
- [14] G. Fricke, C. Bernhardt, K. Heilig, L. A. Schaller, L. Schellenberg, E. B. Shera, and C. W. de Jager, *At. Data Nucl. Data Tables* **60**, 177 (1995).
- [15] V. M. Shabaev, *J. Phys. B* **26**, 1103 (1993).
- [16] H. de Vries, C. W. de Jager, and C. de Vries, *At. Data Nucl. Data Tables* **36**, 495 (1987).
- [17] W. R. Johnson and G. Soff, *At. Data Nucl. Data Tables* **33**, 405 (1985).
- [18] J. D. Zumbro, E. B. Shera, Y. Tanaka, C. E. Bemis, Jr., R. A. Nauman, V. M. Hoehn, W. Reuter, and R. M. Steffen, *Phys. Rev. Lett.* **53**, 1888 (1984); J. D. Zumbro, R. A. Naumann, M. V. Hoehn, W. Reuter, E. B. Shera, C. E. Bemis, Jr., and Y. Tanaka, *Phys. Lett. B* **167**, 383 (1986).
- [19] T. Franosch and G. Soff, *Z. Phys. D* **18**, 219 (1991).
- [20] A. N. Artemyev, T. Beier, G. Plunien, V. M. Shabaev, G. Soff, and V. A. Yerokhin, *Phys. Rev. A* **60**, 45 (1999).
- [21] W. R. Johnson, S. A. Blundell, and J. Sapirstein, *Phys. Rev. A* **37**, 307 (1988).
- [22] G. Soff and P. J. Mohr, *Phys. Rev. A* **38**, 5066 (1988).